

TESTING THE DARK ENERGY WITH GRAVITATIONAL LENSING STATISTICS

SHUO CAO^{1,2}, GIOVANNI COVONE^{2,3} AND ZONG-HONG ZHU¹
Draft version September 13, 2018

ABSTRACT

We study the redshift distribution of two samples of early-type gravitational lenses, extracted from a larger collection of 122 systems, to constrain the cosmological constant in the Λ CDM model and the parameters of a set of alternative dark energy models (XCDM, Dvali-Gabadadze-Porrati and Ricci dark energy models), in a spatially flat universe. The likelihood is maximized for $\Omega_\Lambda = 0.70 \pm 0.09$ when considering the sample excluding the Sloan Lens ACS systems (known to be biased toward large image-separation lenses) and no-evolution, and $\Omega_\Lambda = 0.81 \pm 0.05$ when limiting to gravitational lenses with image separation $\Delta\theta > 2''$ and no-evolution. In both cases, results accounting for galaxy evolution are consistent within 1σ . The present test supports the accelerated expansion, by excluding the null hypothesis (i.e., $\Omega_\Lambda = 0$) at more than 4σ , regardless of the chosen sample and assumptions on the galaxy evolution. A comparison between competitive world models is performed by means of the Bayesian information criterion. This shows that the simplest cosmological constant model that has only one free parameter is still preferred by the available data on the redshift distribution of gravitational lenses. We perform an analysis of the possible systematic effects, finding that the systematic errors due to sample incompleteness, galaxy evolution and model uncertainties approximately equal the statistical errors, with present-day data. We find that the largest sources of systemic errors are the dynamical normalization and the high-velocity cutoff factor, followed by the faint-end slope of the velocity dispersion function.

Keywords: cosmology: cosmological parameters — gravitational lensing: strong — methods: statistical

1. INTRODUCTION

In the last 15 years, several complementary observational probes on cosmological scales have found strong evidence for an accelerating expansion of the universe: distance measurements of distant Type Ia supernovae (SNe Ia; Riess et al. (1998); Perlmutter et al. (1999)), the observations of the cosmic microwave background anisotropies (WMAP; Bennett et al. (2003)), and the baryon acoustic oscillations (BAOs) in the power spectrum of matter extracted from galaxy catalogs (Percival et al. 2007). By assuming General Relativity, a negative pressure component has been invoked as the most suitable mechanism for the observed acceleration, the simplest way of which is the cosmological constant Λ , with a constant equation-of-state (EoS) parameter $w = -1$. Dynamical dark energy models have also been proposed in the literature, such as the quintessence (Ratra & Peebles 1988; Caldwell et al. 1998), phantom (Caldwell et al. 2002), quintom (Feng et al. 2005, 2006; Guo et al. 2005), Dvali-Gabadadze-Porrati (DGP) (Dvali et al. 2000; Zhu & Alcaniz 2005; Zhu & Sereno 2008), and Ricci dark energy (RDE) models (Gao et al. 2009; Li et al. 2010).

The existence of a large number of theoretical models has triggered a variety of observational tests, based, for instance, on the angular size-redshift data of compact radio sources (Alcaniz 2002; Zhu & Fujimoto 2002),

the age-redshift relation (Alcaniz et al. 2003), the lookback time to galaxy clusters (Pires et al. 2006), X-ray luminosities of galaxy clusters, and the Hubble parameter data (Gaztañaga et al. 2009; Stern et al. 2010; Cao, Zhu & Liang 2011; Cao, Liang & Zhu 2011). In this context, strong gravitational lensing plays an important role, providing cosmological tests, such as gravitational lensing statistics (Kochanek 1996a; Zhu 1998; Cooray & Huterer 1999; Chiba & Yoshii 1999; Chae et al. 2002; Sereno 2005; Biesiada, Piórkowska, & Malec 2010; Cao, Zhu & Zhao 2011; Cao & Zhu 2012; Cao et al. 2012), Einstein rings in galaxy-quasar systems (Yamamoto & Futamase 2001), clusters of galaxies acting as lenses on background high redshift galaxies (Sereno 2002; Sereno & Longo 2004), and time delay measurements (Schechter 2004). Results from techniques based on gravitational lensing are complementary to other methods and can provide restrictive limits on the cosmological parameters. In this paper we focus on one interesting lensing statistic suggested by Kochanek (1992) and further discussed and developed in literature (e.g., Helbig & Kayser (1996), Ofek, Rix & Maoz (2003)).

Fukugita, Futamase, & Kasai (1990) (but see also Nemiroff (1989)) demonstrated that the gravitational lens expected redshift increases with a larger cosmological constant, Ω_Λ . Kochanek (1992) derived the probability distribution of the redshift of the lens, as a function of the cosmological parameters, at fixed image separation and source redshift. His analysis of a small sample of four lenses strongly favored a null cosmological constant with respect to models with large Ω_Λ in a flat cosmological model. Helbig & Kayser (1996) further discussed the method, assuming no evolution of the galaxy

¹Department of Astronomy, Beijing Normal University, 100875, Beijing, China

²Dipartimento di Scienze Fisiche, Università di Napoli "Federico II", Via Cinthia, I-80126 Napoli, Italy

³INFN Sez. di Napoli, Compl. Univ. Monte S. Angelo, Via Cinthia, I-80126 Napoli, Italy

population and no detection of lensing galaxies beyond a given magnitude. Successively, Kochanek (1996a) extended his analysis to include gravitational lenses with not measured redshift, in order to account for the selection effects. He obtained the upper limit $\Omega_\Lambda < 0.9$ at the 95% CL, assuming a flat cosmological model. Ofek, Rix & Maoz (2003) presented a new analysis of expected lens redshift distribution, taking into account number and mass evolution of the lens population, and applied this method to constrain both the cosmological and mass-evolution parameter spaces. They could obtain a strong upper limit on the cosmological constant ($\Omega_\Lambda < 0.89$ at the 95% CL), in a flat universe with no lens evolution.

Compared with other related methods based on the full lensing probability distribution, all of the uncertainties in the absolute value of the optical depth can be eliminated in the differential probability of Kochanek (1992), since it is determined by integrating the full lensing probability distribution over lens redshifts. Moreover, the sharp cutoff of this relative probability at high redshift makes the quantity $d\tau/dz_l(\Delta\theta, z_s)$ a more powerful cosmological probe (Ofek, Rix & Maoz 2003).

Following works investigating the evolving lens population have concluded that galaxy evolution is not strongly constrained by the redshift distribution test and does not significantly affect lensing statistics (Mitchell et al. 2005; Capelo & Natarajan 2007; Oguri et al. 2012). However, the evolution of mass and number density can introduce large statistical errors and bias in the analysis of the lens redshift distribution. Therefore, it is mandatory to consider the mass and density evolution into the statistical analysis of the redshift distribution of gravitational lenses. Other limitations include systematic effects due to a sample of gravitational lenses which completeness might be not homogenous as a function of the lensed image separation and the lens redshift (Capelo & Natarajan 2007).

Oguri et al. (2012) have presented a comprehensive statistical analysis of the sample of 19 lensed quasars found in the Sloan Digital Sky Survey (SDSS) Quasar Lens Survey (QLS). This sample is used to determine both the cosmological constant and evolution of the massive lensing galaxies. When considering a no-evolution case, a null cosmological constant is rejected at 6σ level, providing an independent evidence for the accelerated expansion.

The purpose of this paper is to extend our previous statistical analysis based on the angular separation distribution of the lensed images (Cao, Zhu & Zhao 2011) by using the redshift distribution test to obtain novel constraints on the parameters of spatially flat cosmological models. With this aim, we use a large sample of 122 gravitational lenses drawn from the Sloan Lens ACS (SLACS) Survey and other sky surveys.

The first aim is to obtain new constraints on the cosmological constant, by assessing both statistical and systematic uncertainties, mainly due to galaxy evolution and sample selection. Then, we also compare a number of alternative dark energy models with different numbers of parameters, in our analysis we apply, following Davis et al. (2007); Li et al. (2010), a model comparison statistic, i.e., the so-called Bayesian information criterion (BIC; (Schwarz 1978)).

With respect to recent works (Oguri et al. 2012), we use a larger, not homogeneous sample and focus our attention on the determination of the cosmological constant and the comparison with other alternative dark energy models, as the current sample size does not allow a firm determination of the rate of mass and number evolution of massive galaxies.

The paper is organized as follows. In Section 2, the basics of gravitational lensing statistics is introduced, also allowing for number and mass evolution of the lens population. We conduct a literature survey for known systems, listing their basic parameters and defining two statistical samples to perform the redshift test. In Section 3, we introduce four cosmological models, and show the results of constraining cosmological parameters using the Markov Chain Monte Carlo method, with and without galaxy evolution. In Section 4, we assess the possible presence of selection effects and systematic biases in our galaxy sample. Finally, we present the main conclusions and discussion in Section 5.

2. THE REDSHIFT TEST AND THE SAMPLE

Following Ofek, Rix & Maoz (2003), the differential optical depth per unit redshift is

$$\frac{d\tau}{dz_l} = n(\Delta\theta, z_l)(1+z_l)^3 S_{\text{cr}} \frac{cdt}{dz_l}, \quad (1)$$

where $n(\theta, z_l)$ is the comoving number density and S_{cr} is the strong lensing cross-section.

Early-type galaxies are accurately described as singular isothermal spheres (SIS), and it is shown that radial mass distribution and ellipticity of the lens galaxy are unimportant in altering the cosmological constraints (Maoz & Rix 1993; Kochanek 1996b). The SIS density profile is

$$\rho(r) = \frac{\sigma^2}{2\pi G} \frac{1}{r^2}, \quad (2)$$

where σ is the velocity dispersion and r is the projected distance from the center. In Section 4, we will discuss the systematic uncertainties introduced by this assumption. The corresponding strong lensing cross-section is

$$S_{\text{cr}} = 16\pi^3 \left(\frac{\sigma}{c}\right)^4 \left(\frac{D_l D_{ls}}{D_s}\right)^2, \quad (3)$$

where D_l , D_s , and D_{ls} are the angular diameter distances between the observer and the lens, the lens and the source and the observer and the source, respectively. Under a Friedman-Walker metric with null space curvature, the angular diameter distance reads

$$D_A(z_1, z_2; \mathbf{p}) = \frac{c}{H_0(1+z_2)} \int_{z_1}^{z_2} \frac{dz'}{E(z'; \mathbf{p})}, \quad (4)$$

where H_0 is the Hubble constant and $E(z; \mathbf{p})$ is the dimensionless expansion rate dependent on redshift z and cosmological model parameters \mathbf{p} . The two multiple images will form at an angular separation

$$\Delta\theta = 8\pi \left(\frac{\sigma}{c}\right)^2 \frac{D_{ls}}{D_s}. \quad (5)$$

We use the empirically determined velocity dispersion distribution function (VDF) of early-type galaxies: following previous works, our sample are limited to lensing

early-type galaxies. The VDF is generally modeled by a modified Schechter function as (Sheth et al. 2003)

$$\frac{dn}{d\sigma} = n_* \left(\frac{\sigma}{\sigma_*} \right)^\alpha \exp \left[- \left(\frac{\sigma}{\sigma_*} \right)^\beta \right] \frac{\beta}{\Gamma(\alpha/\beta)} \frac{1}{\sigma}, \quad (6)$$

where α , β , n_* , σ_* are the faint-end slope, high-velocity cutoff, characteristic number density, and velocity dispersion, respectively. In the following analysis we use the results of Choi et al. (2007), who analyzed data from the SDSS Data Release 5 to derive the VDF of early-type galaxies. The best-fit values of those VDF parameters are $n_* = 8.0 \times 10^{-3} h^3 \text{ Mpc}^{-3}$, where h is H_0 in units of $100 \text{ km s}^{-1} \text{ Mpc}^{-1}$, $\sigma_* = 161 \text{ km s}^{-1}$, $\alpha = 2.32 \pm 0.10$, and $\beta = 2.67 \pm 0.07$.

We also allow for evolution of the quantities n_* and σ_* , by adopting the following parameterization:

$$n_*(z_l) = n_*(1+z_l)^P, \sigma_*(z_l) = \sigma_*(1+z_l)^U, \quad (7)$$

where P and U are constant quantities.

In the following, we check the effect of redshift evolution by letting P and U be free parameters in Section 3, instead of adopting the evolution of $(P, U) = (-0.23, -0.01)$ predicted by the semi-analytic model of Kang et al. (2005); Chae (2007). Moreover, since the main goal of this paper is to constrain cosmological parameters, we first consider P and U as free parameters, obtain their best-fit values and probability distribution function, and marginalize them to determine constraints on the relevant cosmological parameters of interest.

Straightforward calculations lead to the optical depth per unit redshift for a system with image separation $\Delta\theta$ and source redshift z_s ,

$$\begin{aligned} \frac{d\tau}{dz_l}(\Delta\theta, z_s) &= \tau_N (1+z_l)^{-U\alpha+P} \\ &\times (1+z_l)^3 \frac{D_{ls}}{D_s} D_l^2 \frac{cdt}{dz_l} \left(\frac{\Delta\theta}{\Delta\theta_*} \right)^{\frac{1}{2}\alpha+1} \\ &\times \exp \left[- \left(\frac{\Delta\theta}{\Delta\theta_*} \right)^{\frac{1}{2}\beta} (1+z_l)^{-U\beta} \right], \end{aligned} \quad (8)$$

where the normalization,

$$\tau_N = 2\pi^2 n_* \frac{\beta}{\Gamma(\alpha/\beta)} \left(\frac{\sigma_*}{c} \right)^2, \quad (9)$$

and

$$\Delta\theta_* = 8\pi \left(\frac{\sigma_*}{c} \right)^2 \frac{D_{ls}}{D_s}. \quad (10)$$

For a given lens system, $d\tau/dz_l$ gives the relative probability of finding the lens at different redshift:

$$\begin{aligned} \delta p_l &= \frac{d\tau}{dz_l} / \tau \\ &= \frac{d\tau}{dz_l} / \int_0^{z_s} \frac{d\tau}{dz_l} dz_l. \end{aligned} \quad (11)$$

Besides the probability of lensing by a deflector at z_l , $d\tau/dz_l$, the total optical depth for multiple imaging τ and the probability that a background source lensed by an SIS galaxy with image separation $\Delta\theta$, $d\tau/d\Delta\theta$ (Cao, Zhu & Zhao 2011; Cao & Zhu 2012), can also be obtained by integrating the differential probability in Equation (8).

Moreover, it should be noted that the image separation is taken into account as a prior in the method applied in this paper, which makes it an advantage to use almost all the known lenses (Kochanek 1992). We have compiled a list of 122 gravitational lenses from a variety of sources in literature. Their basic data (lens and source redshifts both and the largest image separations) are summarized in Table 1. As mentioned above, in order to build an homogeneous galaxy sample, we limit our analysis to galaxies with early-type morphology.

The main source is given by the SLACS project (Bolton et al. 2008), providing 59 lenses in our list. These lenses have redshifts in the range from $z_l \simeq 0.05$ to 0.5, making the lower redshift part of our overall sample, with the lensed sources ranging from $z_s \simeq 0.2$ to 1.2 (Bolton et al. 2008). As a consequence of the initial spectroscopic selection method, all the SLACS gravitational lenses have known spectroscopic redshifts for both source and lens, giving the SLACS sample an immediate scientific advantage over strong-lens candidate samples selected from imaging data. However, it is known that the SLACS sample is biased towards moderately large-separation lenses ($\Delta\theta > 2''$; (Arneson et al. 2012)), leading to biased estimates in the redshift test (Capelo & Natarajan 2007).

A majority of the sample was observed as part of the CASTLES program⁴, but it also contains gravitational lenses found in the COSMOS survey⁵ (Faure et al. 2008) and the Extended Growth Strip (EGS; (Moustakas et al. 2007)), including six additional COSMOS and EGS systems discovered recently: COSMOS5921+0638, COSMOS0056+1226, COSMOS0245+1430, "Cross", and "Dewdrop". Finally, we also include five early-type gravitational lenses from Lenses Structure and Dynamics survey (LSD, (Koopmans & Treu 2002, 2003; Treu & Koopmans 2004)), spanning the redshift range $0.48 < z_l < 1.00$ (Q0047-2808, HST15433+5352, MG2016, CY2201-3201 and CFRS03.1077).

Moreover, lenses dominated by a group or cluster potential will affect the constraint results (Keeton & Zabludoff 2004; Oguri et al. 2005; Faure et al. 2011) and previous versions of the lens redshift test have certainly gone to some effort to exclude these systems. Therefore, systems known to be strongly affected by the presence of a group (e.g., B1359+154) or galaxy cluster (e.g., Q0957+561, SDSS1004+4112, and B2108+213) have been excluded from our sample. Moreover, we adopt the image separation criterion of $4''$ to remove lenses that are influenced by complex environments such as clusters (Ofek, Rix & Maoz 2003). On this basis we have removed Q0047-2828, and RXJ0921+4529 from the final sample. However, it should be noted that this technique is not biased by this criterion, because the redshift of a lens that has a large separation is very low compared with the source redshift (Ofek, Rix & Maoz 2003).

The redshift distribution test requires a statistically complete and well characterized sample. As our list includes galaxies from a variety of surveys, using very different observational strategies and discovery spaces (the SDSS spectroscopic sample, Hubble Space Telescope

⁴ <http://cfa-www.harvard.edu/castles/>

⁵ <http://cosmos.astro.caltech.edu/>

(HST) field sky survey, etc.), it is mandatory to verify the completeness of our final sample of gravitational lenses and its usability for the redshift test. In our analysis, we will use the two following samples (see Table 2).

Sample A. Sixty-three lenses from the above list, excluding the whole SLACS sample. This sample is extracted by the same parent population as the primary sample investigated in Capelo & Natarajan (2007).

Sample B. Seventy-one lenses with image separation larger than $2''$. This choice is motivated by the fact that the SLACS sample is biased toward moderately large-separation lenses and large velocity dispersions and is less than 50% complete below $\Delta\theta = 2''$ (Arneson et al. 2012).

We will discuss the samples selection functions and the impact on our results in Section 4.

3. STATISTICAL ANALYSIS

Our statistical analysis is based on the maximum likelihood technique. For a sample of N_L multiply imaged sources, the likelihood \mathcal{L} of the observed lens redshift given the statistical lensing model is defined by

$$\ln \mathcal{L} = \sum_{l=1}^{N_L} \ln \delta p_l(\mathbf{p}), \quad (12)$$

where $\delta p_l(\mathbf{p})$ is the particular differential probability given by Equation(11) normalized to one, and \mathbf{p} are the cosmological model parameters (e.g., Ω_Λ , Ω_m), for the l th multiply imaged source. Accordingly, the χ^2 is defined as follows:

$$\chi^2 = -2 \ln \mathcal{L}. \quad (13)$$

and the best-fit model parameters are determined by minimizing χ^2 . Our analysis is based on the publicly available package COSMOMC (Lewis & Bridle 2002).

We consider four different cosmological models to be tested with the observed lens redshift distribution: the Λ CDM model and three phenomenological models in which the vacuum energy is described as a dynamical quantity: the so-called XCDM model with the EoS $w = p/\rho$ a free parameter, the DGP model arising from the brane world theory, and the RDE models. These models are motivated by the well known fine-tuning and coincidence problems of the standard Λ CDM model.

We note that the previous precision cosmological observational data have hinted that both the RDE and dark energy with EoS $w < -1$ may have dubious stability problems (Feng & Li 2009; Amani 2011), and the DGP model has already been ruled out observationally (Fang et al. 2008; Durrer & Maartens 2010; Maartens & Koyama 2010), so it is indicated that these are just supposed to be a representative set, instead of viable candidates for dark energy.

It is well known that the χ^2 -statistics alone is not sufficient to provide an effective way to make a comparison between different models. In this paper, we use the BIC as a model selection criterion (Schwarz 1978). The BIC is defined by

$$\text{BIC} = -2 \ln \mathcal{L}_{\max} + k \ln N, \quad (14)$$

where \mathcal{L}_{\max} , k , N are the maximum likelihood, the number of parameters, and the number of data points, respectively. Under this selection criterion, a positive evidence

against the model with the higher BIC is defined by a difference $\Delta\text{BIC} = 2$ and a strong evidence is defined by $\Delta\text{BIC} = 6$.

A spatially flat universe is assumed throughout the paper, which is strongly supported a combined 5-years Wilkinson Microwave Anisotropy Probe (WMAP5), BAOs, and SN data (Hinshaw et al. 2009). As mentioned above, we also consider the case of an evolving population of lensing galaxies in order to assess the accuracy of our results. We consider simultaneous constraints on the galaxy evolution and cosmological parameters. In order to derive the probability distribution function for the cosmological parameters of interest, we marginalize P and U and perform fits of different cosmological scenarios on both Samples A and B. Results are shown in Figure 1 - 6 and summarized in Table 5.

3.1. The standard cosmological model (Λ CDM)

In the simplest scenario, the dark energy is a cosmological constant, Λ , i.e., a component with constant EoS $w = p/\rho = -1$. If spatial flatness of the Friedmann-Robertson-Walker metric is assumed, the Hubble parameter according to the Friedmann equation is

$$H^2 = H_0^2 [\Omega_m (1+z)^3 + \Omega_\Lambda], \quad (15)$$

where Ω_m and Ω_Λ represent the density parameters of matter (both baryonic and non-baryonic components) and cosmological constant, respectively. As $\Omega = \Omega_m + \Omega_\Lambda = 1$, this model has only one independent parameter.

We consider constraints obtained both samples defined above. While considering Sample A, the likelihood is maximized, $\mathcal{L} = \mathcal{L}_{\max}$, for $\Omega_\Lambda = 0.70 \pm 0.09$ with no redshift evolution and $\Omega_\Lambda = 0.73 \pm 0.09$ with redshift evolution, see Figure 1. Hereafter, uncertainties denote the statistical 68.3% confidence limit for one parameter, determined by $\mathcal{L}/\mathcal{L}_{\max} = \exp(-1/2)$. Data are consistent with the no-redshift-evolution case ($P = 0$, $U = 0$) at 1σ . Specifically, the measured values of the two parameters are $P = -1.2 \pm 1.4$ and $U = 0.22_{-0.27}^{+0.26}$.

When using the Sample B, we find, in the no-evolution scenario, $\Omega_\Lambda = 0.81 \pm 0.05$, consistent with the result from Sample A. When allowing for galaxy evolution, we find $\Omega_\Lambda = 0.83 \pm 0.05$, $P = -1.9 \pm 4.6$, and $U = 0.16 \pm 0.30$.

In both cases, our findings are very close to the ones obtained from the ESSENCE supernova survey data, $\Omega_\Lambda = 0.73 \pm 0.04$ in the flat case (Davis et al. 2007), and from the combined WMAP 5-year, BAO, and SN Union data (Komatsu et al. 2009) with the best-fit parameter $\Omega_\Lambda = 0.726 \pm 0.015$. Moreover, both samples used here exclude with large confidence (4σ level) the null hypothesis of a vanishing Ω_Λ , as obtained also by Oguri et al. (2012) in their statistical analysis on the SQLS data, providing independent evidence of the accelerated expansion.

While detailed analysis on the constraints of the redshift distribution test on the hierarchical models of galaxy evolution is beyond the scope of this work, we notice that these results obtained with both samples are in broad agreement with previous studies (Capelo & Natarajan 2007; Oguri et al. 2012), in which no strong evidence for any evolution of the parameters U and P was found. Moreover, we find that the degen-

Table 1

Summary of the Properties of the Strongly Lensed Systems, with the SLACS Lenses Written in Bold. References: 1 - Bolton et al. (2008); 2 - Treu et al. (2006); 3 - Newton et al. (2011); 4 - Ruff et al. (2011); 5 - Koopmans & Treu (2002); 6 - Koopmans & Treu (2003); 7 - Treu & Koopmans (2004); 8 - Kochanek et al. (2000); 9 - Winn et al. (2002b); 10 - Gregg et al. (2002); 11 - Hall et al. (2002); 12 - O’Dea et al. (1992); 13 - Wiklind & Combes (1995); 14 - Cohen et al. (2002); 15 - Crampton et al. (2002); 16 - Falco, Lehar, & Shapiro (1997); 17 - Tonry & Kochanek (1999); 18 - Wisotzki et al. (2002); 19 - Gregg et al. (2000); 20 - Fassnacht & Cohen (1998); 21 - Hagen & Reimers (2000); 22 - Lubin et al. (2000); 23 - Kneib, Cohen, & Hjorth (2000); 24 - Muñoz et al. (2001); 25 - Schechter et al. (1998); 26 - Lehar et al. (2000); 27 - Lacy et al. (2002); 28 - Hewett et al. (1994); 29 - Surdej et al. (1997); 30 - Eisenhardt et al. (1996); 31 - Lidman et al. (2000); 32 - Tonry (1998); 33 - Myers et al. (1999); 34 - Siemiginowska et al. (1998); 35 - Ratnatunga et al. (1999); 36 - Burud et al. (2002b); 37 - Lehar et al. (1993); 38 - Fassnacht et al. (1996); 39 - Winn et al. (2002a); 40 - Morgan et al. (2001); 41 - Langston et al. (1989); 42 - Wiklind & Combes (1996); 43 - Winn et al. (2000); 44 - Sykes et al. (1998); 45 - Fassnacht et al. (1999); 46 - Burud et al. (2002a); 47 - Huchra et al. (1985); 48 - Inada et al. (2005); 49 - Biggs et al. (2003); 50 - Johnston et al. (2003); 51 - Blackburne et al. (2008); 52 - Sluse et al. (2003); 53 - Eigenbrod et al. (2006); 54 - Inada et al. (2008); 55 - Morgan et al. (2004); 56 - Ofek et al. (2006); 57 - Faure et al. (2008); 58 - Anguita et al. (2009); 59 - Lagattuta et al. (2010); 60 - Moustakas et al. (2007).

| Lens Name | z_s | z_l | $\Delta\theta('')$ | Ref | Lens Name | z_s | z_l | $\Delta\theta('')$ | Ref |
|-------------------|--------|--------|--------------------|-------|------------------|--------|---------|--------------------|----------|
| J0029-0055 | 0.9313 | 0.227 | 1.92 | 1 | J221929-001743 | 1.0232 | 0.2888 | 1.472 | 4 |
| J0037-0942 | 0.6322 | 0.1955 | 2.943 | 1,2 | J022511-045433 | 1.1988 | 0.2380 | 3.54 | 4 |
| J0044+0113 | 0.1965 | 0.1196 | 1.58 | 1,3 | J022610-042011 | 1.232 | 0.4943 | 2.306 | 4 |
| J0109+1500 | 0.5248 | 0.2939 | 1.38 | 1 | MG2016 | 3.263 | 1.004 | 3.12 | 5 |
| J0216-0813 | 0.5235 | 0.3317 | 2.303 | 1,2,3 | HST15433+5352 | 2.092 | 0.497 | 1.18 | 5,6,7 |
| J0252+0039 | 0.9818 | 0.2803 | 2.08 | 1 | CY2201-3201 | 3.900 | 0.320 | 0.830 | 5,6,7 |
| J0330-0020 | 1.0709 | 0.3507 | 2.2 | 1,3 | CFRS03.1077 | 2.941 | 0.938 | 2.48 | 5,6,7 |
| J0405-0455 | 0.8098 | 0.0753 | 1.6 | 1 | Q0142-100 | 2.72 | 0.49 | 2.231 | 8 |
| J0728+3835 | 0.6877 | 0.2058 | 2.5 | 1 | PMNJ0134-0931 | 2.216 | 0.76451 | 0.7 | 9,10,11 |
| J0737+3216 | 0.5812 | 0.3223 | 2.065 | 2,3 | B0218+357 | 0.944 | 0.685 | 0.33 | 12,13,14 |
| J0822+2652 | 0.5941 | 0.2414 | 2.34 | 1 | CFRS03.1077 | 2.941 | 0.938 | 2.1 | 15 |
| J0841+3824 | 0.6567 | 0.1159 | 2.82 | 1 | MG0414+0534 | 2.64 | 0.9584 | 2.12 | 16,17 |
| J0912+0029 | 0.3239 | 0.1642 | 3.23 | 1,2 | HE0435-1223 | 1.689 | 0.4 | 2.6 | 18 |
| J0935-0003 | 0.467 | 0.3475 | 1.74 | 1,3 | HE0512-3329 | 1.565 | 0.9313 | 0.644 | 19 |
| J0936+0913 | 0.588 | 0.1897 | 2.18 | 1 | B0712+472 | 1.339 | 0.406 | 1.28 | 20 |
| J0946+1006 | 0.6085 | 0.2219 | 2.76 | 1 | MG0751+2716 | 3.200 | 0.3502 | 0.7 | 17 |
| J0955+0101 | 0.3159 | 0.1109 | 1.82 | 1 | HS0818+1227 | 3.115 | 0.39 | 2.55 | 21 |
| J0956+5100 | 0.4699 | 0.2405 | 2.642 | 1,2 | SBS0909+523 | 1.377 | 0.830 | 1.10 | 22 |
| J0959+4416 | 0.5315 | 0.2369 | 1.92 | 1,2 | RXJ0911+0551 | 2.80 | 0.77 | 3.25 | 23 |
| J0959+0410 | 0.535 | 0.126 | 1.995 | 1 | FBQ0951+2635 | 1.24 | 0.25 | 1.10 | 25 |
| J1016+3859 | 0.4394 | 0.1679 | 2.18 | 1 | BRI0952-0115 | 4.50 | 0.41 | 0.99 | 26 |
| J1020+1122 | 0.553 | 0.2822 | 2.4 | 1 | J100424.9+122922 | 2.65 | 0.95 | 1.54 | 27 |
| J1023+4230 | 0.696 | 0.1912 | 2.82 | 1 | LBQS1009-0252 | 2.74 | 0.88 | 1.53 | 28 |
| J1029+0420 | 0.6154 | 0.1045 | 2.02 | 1 | Q1017-207 | 2.545 | 1.085 | 0.849 | 29 |
| J1032+5322 | 0.329 | 0.1334 | 2.06 | 1 | FSC10214+4724 | 2.286 | 0.914 | 1.59 | 30 |
| J1103+5322 | 0.7353 | 0.1582 | 2.04 | 1,3 | B1030+071 | 1.535 | 0.599 | 1.56 | 20 |
| J1106+5228 | 0.4069 | 0.0955 | 2.46 | 1,3 | HE1104-1805 | 2.32 | 0.729 | 3.19 | 31 |
| J1112+0826 | 0.6295 | 0.273 | 2.98 | 1,3 | PG1115+080 | 1.72 | 0.311 | 2.42 | 32 |
| J1134+6027 | 0.4742 | 0.1528 | 2.2 | 1 | B1152+200 | 1.019 | 0.439 | 1.56 | 33 |
| J1142+1001 | 0.5039 | 0.2218 | 1.96 | 1,3 | Q1208+101 | 3.80 | 1.1349 | 0.47 | 34 |
| J1143-0144 | 0.4019 | 0.106 | 3.36 | 1 | HST14113+5211 | 2.811 | 0.465 | 2.26 | 22 |
| J1153+4612 | 0.8751 | 0.1797 | 2.1 | 1 | HST14176+5226 | 3.40 | 0.81 | 3.25 | 35 |
| J1204+0358 | 0.6307 | 0.1644 | 2.62 | 1,3 | B1422+231 | 3.62 | 0.339 | 1.28 | 32 |
| J1205+4910 | 0.4808 | 0.215 | 2.44 | 1 | SBS1520+530 | 1.855 | 0.717 | 1.568 | 8,36 |
| J1213+6708 | 0.6402 | 0.1229 | 2.84 | 1,3 | MG1549+3047 | 1.17 | 0.11 | 2.3 | 37 |
| J1218+0830 | 0.7172 | 0.135 | 2.9 | 1,3 | B1600+434 | 1.589 | 0.4144 | 1.38 | 20 |
| J1250+0523 | 0.7953 | 0.2318 | 2.26 | 1,2 | B1608+656 | 1.394 | 0.630 | 2.27 | 38 |
| J1330-0148 | 0.7115 | 0.0808 | 1.706 | 1,2 | PMNJ1632-0033 | 3.424 | 1.0 | 1.47 | 39 |
| J1402+6321 | 0.4814 | 0.2046 | 2.775 | 1,2 | FBQ1633+3134 | 1.52 | 0.684 | 0.66 | 40 |
| J1403+0006 | 0.473 | 0.1888 | 1.66 | 1 | MG1654+1346 | 1.74 | 0.254 | 2.1 | 41 |
| J1416+5136 | 0.8111 | 0.2987 | 2.74 | 1,3 | PKS1830-211 | 2.51 | 0.886 | 0.99 | 42 |
| J1420+6019 | 0.5351 | 0.0629 | 2.097 | 1,2 | PMNJ1838-3427 | 2.78 | 0.31 | 1.00 | 43 |
| J1430+4105 | 0.5753 | 0.285 | 3.04 | 1 | B1933+507 | 2.63 | 0.755 | 1.00 | 44 |
| J1432+6317 | 0.6643 | 0.123 | 2.52 | 1,3 | B2045+265 | 1.28 | 0.8673 | 2.2 | 45 |
| J1436-0000 | 0.8049 | 0.2852 | 2.24 | 1,3 | HE2149-2745 | 2.03 | 0.50 | 1.69 | 8, 46 |
| J1443+0304 | 0.4187 | 0.1338 | 1.62 | 1,3 | Q2237+0305 | 1.695 | 0.0394 | 1.82 | 47 |
| J1451-0239 | 0.5203 | 0.1254 | 2.08 | 1,3 | SDSS0246-0825 | 1.68 | 0.724 | 1.2 | 48 |
| J1525+3327 | 0.7173 | 0.3583 | 2.62 | 1,3 | B0850+054 | 3.93 | 0.59 | 0.68 | 49 |
| J1531-0105 | 0.7439 | 0.1596 | 3.42 | 1,3 | SDSS0903+5028 | 3.605 | 0.388 | 3.0 | 50 |
| J1538+5817 | 0.5312 | 0.1428 | 2 | 1,3 | HE1113-0641 | 1.235 | 0.75 | 0.88 | 51 |
| J1621+3931 | 0.6021 | 0.2449 | 2.58 | 1,3 | Q1131-1231 | 0.658 | 0.295 | 3.8 | 52 |
| J1627-0053 | 0.5241 | 0.2076 | 2.42 | 1,2 | SDSS1138+0314 | 2.44 | 0.45 | 1.34 | 53, 54 |
| J1630+4520 | 0.7933 | 0.2479 | 3.618 | 1,2 | SDSS1155+6346 | 2.89 | 0.176 | 1.96 | 55 |
| J1636+4707 | 0.6745 | 0.2282 | 2.18 | 1 | SDSS1226-0006 | 1.12 | 0.52 | 1.26 | 53, 54 |
| J2238-0754 | 0.7126 | 0.1371 | 2.54 | 1,3 | WFI2033-4723 | 1.66 | 0.66 | 2.34 | 53, 55 |
| J2300+0022 | 0.4635 | 0.2285 | 2.494 | 1,2 | HE0047-1756 | 1.66 | 0.41 | 1.54 | 56 |
| J2303+1422 | 0.517 | 0.1553 | 3.278 | 1,2 | COSMOS5921+0638 | 3.15 | 0.551 | 1.6 | 57, 58 |
| J2321-0939 | 0.5324 | 0.0819 | 3.2 | 1,2 | COSMOS0056+1226 | 0.81 | 0.361 | 2.4 | 57, 59 |
| J2341+0000 | 0.807 | 0.186 | 2.88 | 1,3 | COSMOS0245+1430 | 0.779 | 0.417 | 3.08 | 57,59 |
| J021737-051329 | 1.847 | 0.6458 | 2.536 | 4 | "Cross" | 3.40 | 0.810 | 2.44 | 60 |
| J141137+565119 | 1.420 | 0.3218 | 1.848 | 4 | "Dewdrop" | 0.982 | 0.580 | 1.52 | 60 |

Table 2

Summary of the Subsamples Used in the Analysis of This Paper.

| Subsample | Definition |
|-------------|---|
| Sample A | 63 lenses from Table 1 excluding the SLACS sample |
| Sample B | 71 lenses with image separation larger than $2''$ |
| Sample C | 51 lenses with image separation not larger than $2''$ |
| SLACS | 59 lenses from the whole SLACS sample |
| Full sample | 122 lenses from Table 1 |

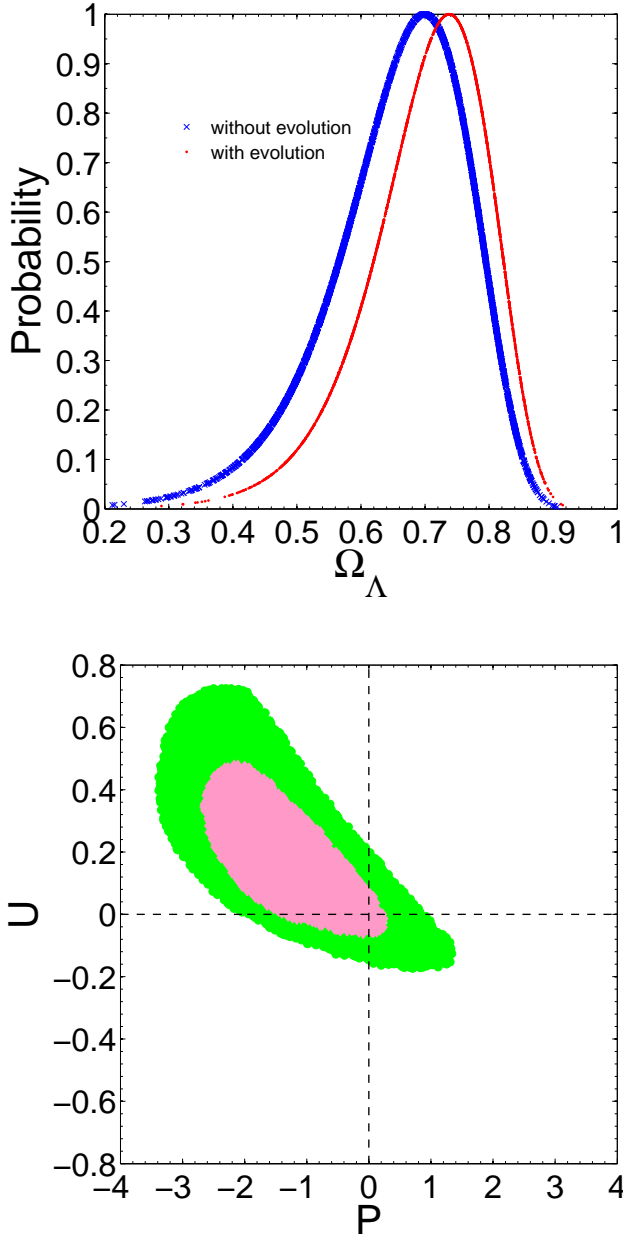


Figure 1. Simultaneous constraints on the cosmological constant and VDF evolutions in the flat Λ CDM model obtained by using Sample A. Upper panel: likelihood distributions as a function of Ω_Λ with and without redshift evolution. The red dotted line is obtained after marginalizing over P and U . Lower panel: constraints on P and U after marginalizing over Ω_Λ . Dashed lines in the lower panel represent the case without redshift evolution ($P = U = 0$).

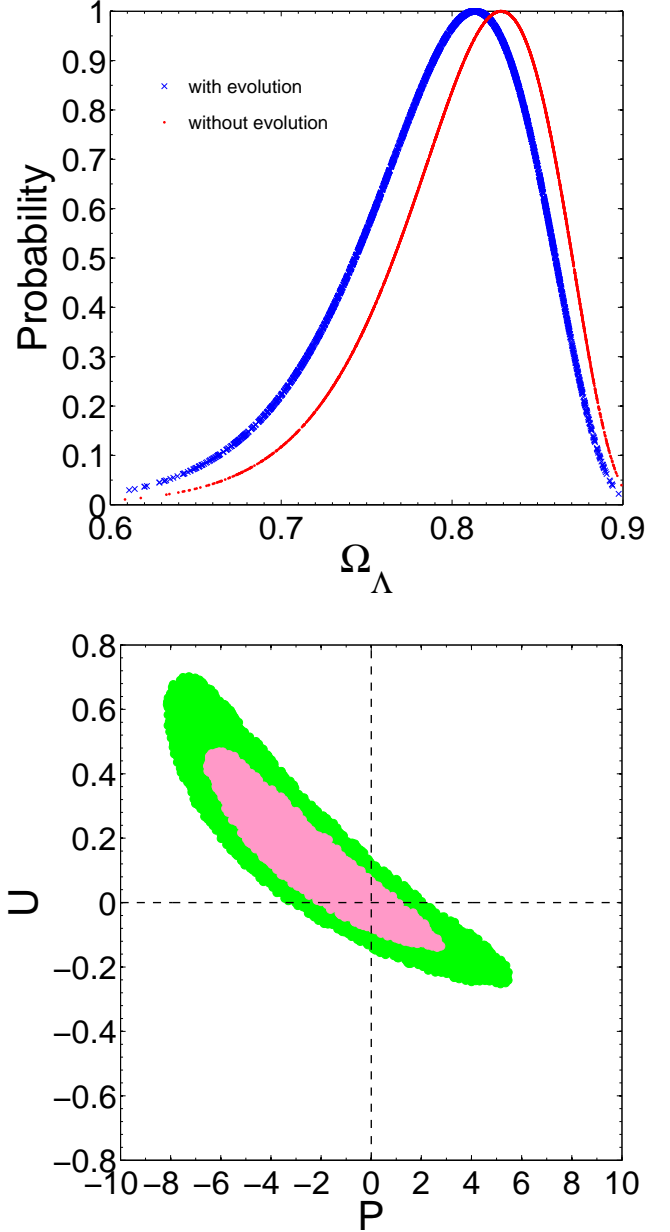


Figure 2. As in Figure 1, using Sample B (i.e., lensing systems with image separation larger than $2''$).

erate direction in the evolution parameters corresponds to a constant lensing probability, as already been noted by Oguri et al. (2012).

Previous studies on lensing statistics (Chae 2003; Ofek, Rix & Maoz 2003) considering a not-evolving velocity dispersion function have obtained consistent results with the galaxy number counts (Im et al. 2002). Mitchell et al. (2005); Capelo & Natarajan (2007) assumed a non-evolving shape for the VDF and obtained results consistent with earlier results. To sum up, all previous results on redshift evolution from strong lensing statistics appear to be in agreement with no-evolution of early-type galaxies. As we only considered early-type lensing galaxies, our results further confirm this conclusion.

Substantial evolution of galaxy number (i.e, $P \simeq -1$)

and mass (i.e., $U \simeq 0.25$) are supported by studies of early-type galaxies from $z = 1$ to 0 (Faber et al. 2007; Brown et al. 2007; Oguri et al. 2012) This conclusion is consistent with our results in Section 3.

3.2. Constraints on selected dark energy models

Now we focus on the constraints obtained on selected dark energy models. Here, we only use Sample A, as results obtained with Sample B are coherent at 1σ level.

3.2.1. Dark energy with constant equation of state (XCDM)

While deviating from the simple case $w = -1$, the EoS of dark energy $w < -1/3$ can also give birth to an accelerated universe expansion. In a zero-curvature universe, the Hubble parameter reads:

$$H^2 = H_0^2[\Omega_m(1+z)^3 + \Omega_x(1+z)^{3(1+w)}]. \quad (16)$$

Obviously, when flatness is assumed ($\Omega_m + \Omega_\Lambda = 1$), it is a two-parameter cosmological model, $\mathbf{p} = \{\Omega_x, w\}$.

The best-fit values of the parameters are: $\Omega_x = 0.77 \pm 0.17$; $w = -2.3_{-2.7}^{+1.3}$ with no redshift evolution and $\Omega_x = 0.79 \pm 0.13$; $w = -2.1_{-2.8}^{+1.1}$ with redshift evolution, see Figure 3 and Figure 4 for the confidence limits in the $\Omega_x - w$ plane. However, we note that the lower limits on the parameter w are probably an artifact of the prior $w > -5$, which may be tested and constrained with future larger lens sample. Also in this cosmological scenario, the lens redshift data are consistent with no redshift evolution: when marginalizing over Ω_x , we find $P = -1.4 \pm 1.4$ and $U = 0.20 \pm 0.28$. The Einstein's cosmological constant ($w = -1$) is still consistent within 1σ . Meanwhile, compared to the cosmological constant model, this flat cosmology with constant EoS dark energy provides a lower χ_{min}^2 , but a higher BIC: $\Delta\text{BIC} = 1.72$ with no redshift evolution and $\Delta\text{BIC} = 1.55$ with redshift evolution. However, we note that comparing with the cosmological constant model, the two-parameter XCDM model performs relatively well under the information criterion test.

3.2.2. Dvali-Gabadadze-Porrati model (DGP)

In a brane world theory, the accelerated expansion of the universe can be explained by the gravity leaking out into the bulk at large scales with a crossover scale (Dvali et al. 2000). The Friedmann equation is

$$3M_{\text{Pl}}^2 \left(H^2 - \frac{H}{r_c} \right) = \rho_m(1+z)^3, \quad (17)$$

where M_{Pl} is the Planck mass and $r_c = (H_0(1 - \Omega_m))^{-1}$ is the crossover scale at which the induced 4-dimensional Ricci scalar dominates. In this model, the Hubble parameter expresses as

$$H^2 = H_0^2(\sqrt{\Omega_m(1+z)^3 + \Omega_{r_c}} + \sqrt{\Omega_{r_c}})^2, \quad (18)$$

and the DGP model has one free parameter $\mathbf{p} = \{\Omega_m\}$ in a flat universe.

For the DGP model, the best-fit parameters are $\Omega_m = 0.25_{-0.09}^{+0.11}$ with no redshift evolution and $\Omega_m = 0.22_{-0.09}^{+0.10}$ with redshift evolution (See Figure 5). We find that the DGP model is somehow worse than the Λ CDM model with this observational data. While its χ_{min}^2 is larger

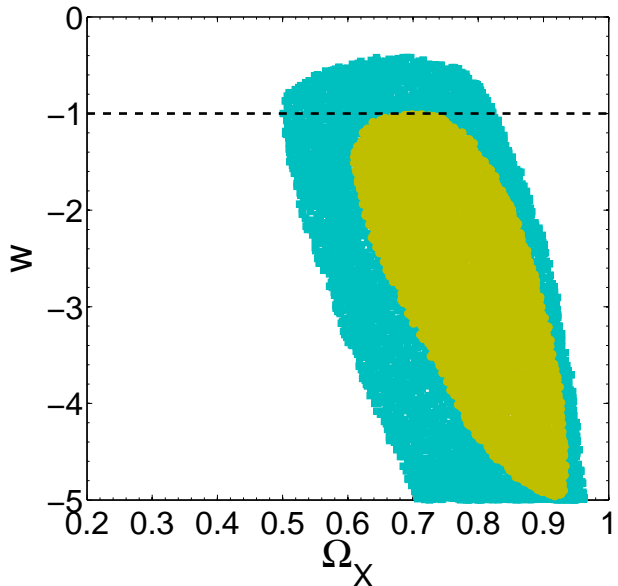


Figure 3. Likelihood contours for the flat XCDM model at 68.3% and 95.4% CL in the $\Omega_x - w$ plane obtained by using Sample A with no redshift evolution. The lower limit on w is probably an artifact of the prior $w > -5$ and the horizontal dotted line indicates a cosmological constant with $w = -1$.

than that of the Λ CDM model by about 1.2, it gives $\Delta\text{BIC} = 1.20$ with no redshift evolution and $\Delta\text{BIC} = 1.19$ with redshift evolution.

3.2.3. Ricci dark energy (RDE) model

Following Gao et al. (2009); Li et al. (2010), the average radius of the Ricci scalar curvature $|\mathcal{R}|^{-1/2}$ might provide an infrared cutoff length scale. Accordingly, the DE energy density is

$$\rho_{de} = 3\beta^2(\dot{H} + 2H^2), \quad (19)$$

and the Hubble parameter reads

$$H^2 = H_0^2 \left[\frac{2\Omega_m}{2-\beta}(1+z)^3 + \left(1 - \frac{2\Omega_m}{2-\beta}\right)(1+z)^{(4-\frac{2}{\beta})} \right] \quad (20)$$

where β is a positive constant to be determined. This is a two-parameter model with $\mathbf{p} = \{\Omega_m, \beta\}$.

For the RDE model, the best-fit values of the parameters are $\Omega_m = 0.22_{-0.11}^{+0.10}$; $\beta = 0.29 \pm 0.19$ with no redshift evolution, and $\Omega_m = 0.18_{-0.12}^{+0.11}$; $\beta = 0.28 \pm 0.18$ with redshift evolution. In Figure 6, we plot the likelihood contours in the $\Omega_m - \beta$ plane. Given the largest information criterion result: $\Delta\text{BIC} = 1.78$ with no redshift evolution, and $\Delta\text{BIC} = 1.62$ with redshift evolution, the RDE model performs the worst in all the cosmological models considered in this paper.

4. BIASES AND POSSIBLE SYSTEMATIC EFFECTS

Thus far we have considered only statistical errors. Indeed, cosmological tests based on strong lensing have been somehow controversial since Kochanek (1996a), in particular for the possible biases associated with sample selection (Capelo & Natarajan 2007). In this section, we discuss several possible sources of systematic errors, including: sample incompleteness, unknown survey selec-

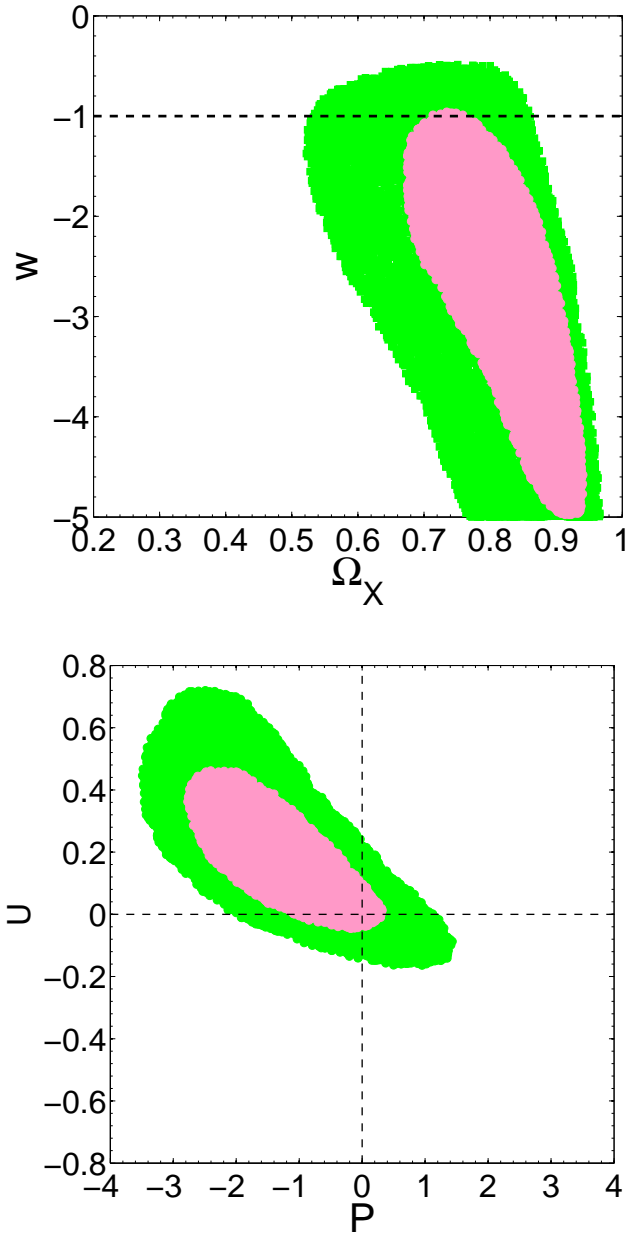


Figure 4. As in Figure 1, but for the flat XCDM model obtained by using Sample A with redshift evolution. The lower limit on w is probably an artifact of the prior $w > -5$ and the horizontal dotted line indicates a cosmological constant with $w = -1$.

tion function, uncertainties in the lensing galaxy properties and lens modeling, in order to verify their effect on the cosmological constraints.

First of all, one general concern is given by the fact that strong gravitational lenses are a biased sample of galaxies. Most of the previous works found no evidence for a biased sample of the lensing population with respect to massive early-type galaxies (see, e.g., Treu et al. (2006)). On the other hand, Faure et al. (2011) found possible evidence for the stellar mass of lensing early-type galaxies to evolve significantly with redshift. However, it is still not clear whether this supports a stronger lensing bias toward massive objects at high redshift or if it is a consequence of the possible higher proportion of massive

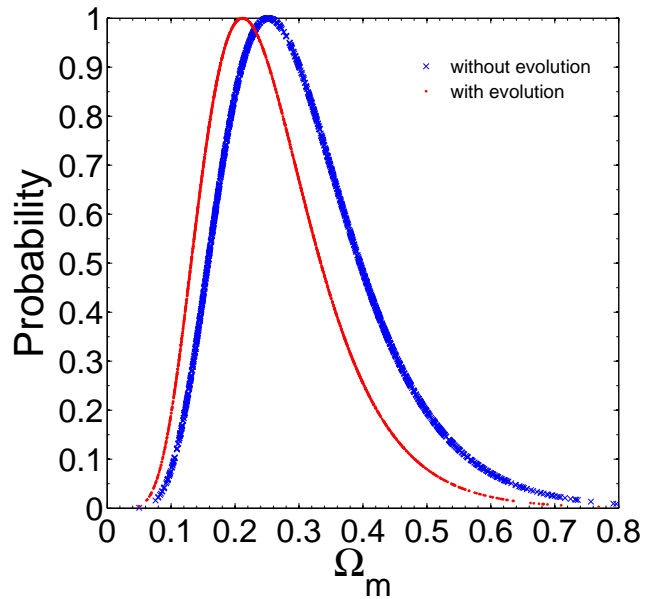


Figure 5. Normalized likelihood as a function of Ω_m for the DGP model obtained by using Sample A with and without redshift evolution.

and high stellar density galaxies at high redshift. This could be addressed in dedicated numerical simulations (van de Ven et al. 2009; Mandelbaum et al. 2009), as the available lens samples cannot allow yet to discriminate between the two alternatives.

We now estimate the systematic errors due to statistical sample incompleteness. As both our Samples (A, B) have been put together from different surveys, differences in the observing strategies (and selection functions) may cause systematic errors hard to estimate. In order to evaluate the effects due to a selection bias, we have re-derived the best estimate on Ω_Λ (with a no-evolving lens population) by using the whole catalog of $n = 122$ lenses and two additional, smaller samples (see Table 2): the first one includes only galaxies from the SLACS, and the second one the gravitational lenses with separations not larger than $2''$, including 59 and 51 systems, respectively. All of these three samples clearly suffer from strong selection effects or are very inhomogeneous and are therefore not suitable for deriving constraints by means of the redshift distribution test. However, they can shed light on the amplitude of the possible systematic errors due to sample inhomogeneity, incompleteness, and selection bias toward non-representative systems. For instance, it is well known that the SLACS catalog is characterized by a selection function favoring moderately massive ellipticals (e.g., Arneson et al. (2012)); also the somehow extreme case of Sample C is not complete (below $\Delta\theta = 2''$) as the probability to detect a lensing galaxy is related to the image separation as very small-separation lenses easily escape detection (both in present-day imaging and spectroscopic surveys). Therefore, we expect that the estimates of Ω_Λ obtained from these samples allow us to establish an upper limit on the systematic errors due to a not well-defined lens sample.

Results are shown in Figure 7. When using the apparently incomplete sample of small separation lenses (Sample C) we find $\Omega_\Lambda = 0.65^{+0.11}_{-0.15}$. This rather smaller value

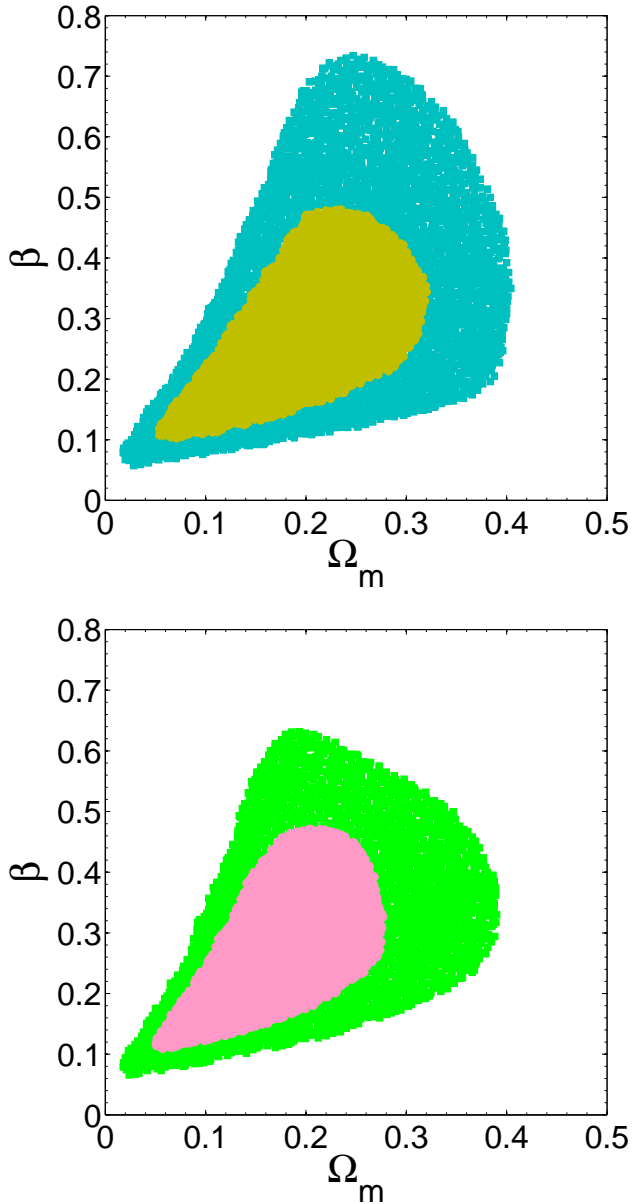


Figure 6. Likelihood contours for the RDE model at 68.3% and 95.4% CL obtained by using Sample A with no redshift evolution (upper) and with redshift evolution (lower).

can be related to the fact that lower-mass lenses, producing small-separation images, will tend to be located at redshifts lower than expected in a large- Ω_Λ model. Hence, this determines a slightly lower value for the cosmological constant.

When adopting the whole SLACS sample, we find $\Omega_\Lambda = 0.73^{+0.14}_{-0.18}$. Finally, by considering the whole, inhomogeneous list of 122 lenses, we obtain $\Omega_\Lambda = 0.71^{+0.07}_{-0.08}$. When we compare these values with the best estimate obtained from Sample A, we note that systematic errors do not exceed ~ 0.1 on the cosmological constant.

We have assumed all the lenses to be isolated systems, with negligible line-of-sight contamination. However, current studies find that proximate galaxies (Cohn & Kochanek 2004) and environmental groups (Keeton & Zabludoff 2004) can have various effects on

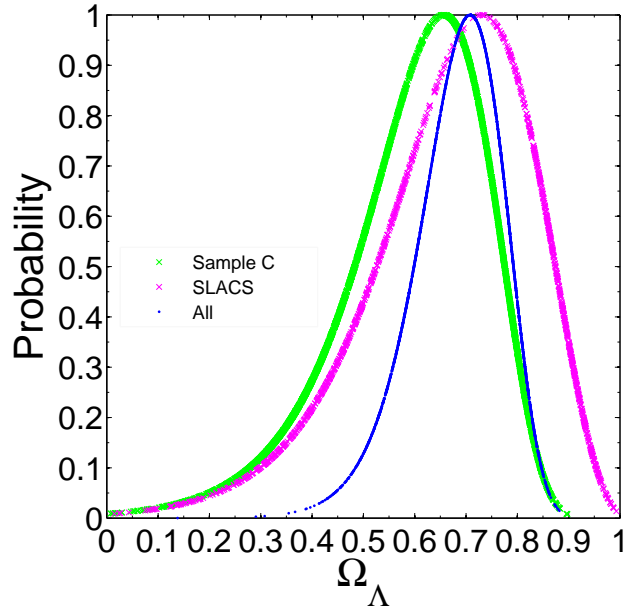


Figure 7. Normalized likelihood plot as a function of Ω_Λ for the flat Λ CDM model, for the three biased samples described in the text.

the primary lens galaxies, even though the most significant effects only appear to be biasing the galaxy ellipticities and image multiplicities. Nevertheless, most of lenses in Sample B come from the SLACS survey where the role of environment has been assessed in Treu et al. (2009). Namely, it was found that for SLACS lenses the typical contribution from external mass distribution is no more than a few percent. Therefore, the environmental effects on observed image separations appear to be relatively small (certainly smaller than statistical errors arising from the current sample size of lenses).

In addition to the main lens galaxy, the contribution from line-of-sight density fluctuations to the lens potential should also be taken into consideration. Based on the final lens sample from SQLS, Oguri et al. (2012) have investigated the line-of-sight effect and found that its effect on the total lensing probability is rather small compared with the contribution of other systematic errors to the systematic error on Ω_Λ (see Table 2 in Oguri et al. (2012)). Meanwhile, it is noted that this effect may also have a larger impact on lensing probabilities for the lens samples with larger images separations (Oguri et al. 2005; Faure et al. 2009).

Evolution of the VDF and model uncertainties can introduce additional systematic errors. Here we estimate these systematic errors on the constraint results of the flat Λ CDM with the full sample ($n = 122$ lenses), in a similar way as done in Oguri et al. (2012). The analysis in Section 3 suggests that unconstrained redshift evolution of the velocity function is one of the most significant sources of systematic error. An additional source of uncertainty is the relation between velocity dispersions and image separations. This uncertainty is not only related to the difference between the velocity dispersion σ_{SIS} of the mass distribution and the observed stellar velocity dispersion σ_0 (White & Davis 1996), but also many complexities such as the velocity dispersion normalization factor for non-spherical galaxies (Oguri et al. 2012)

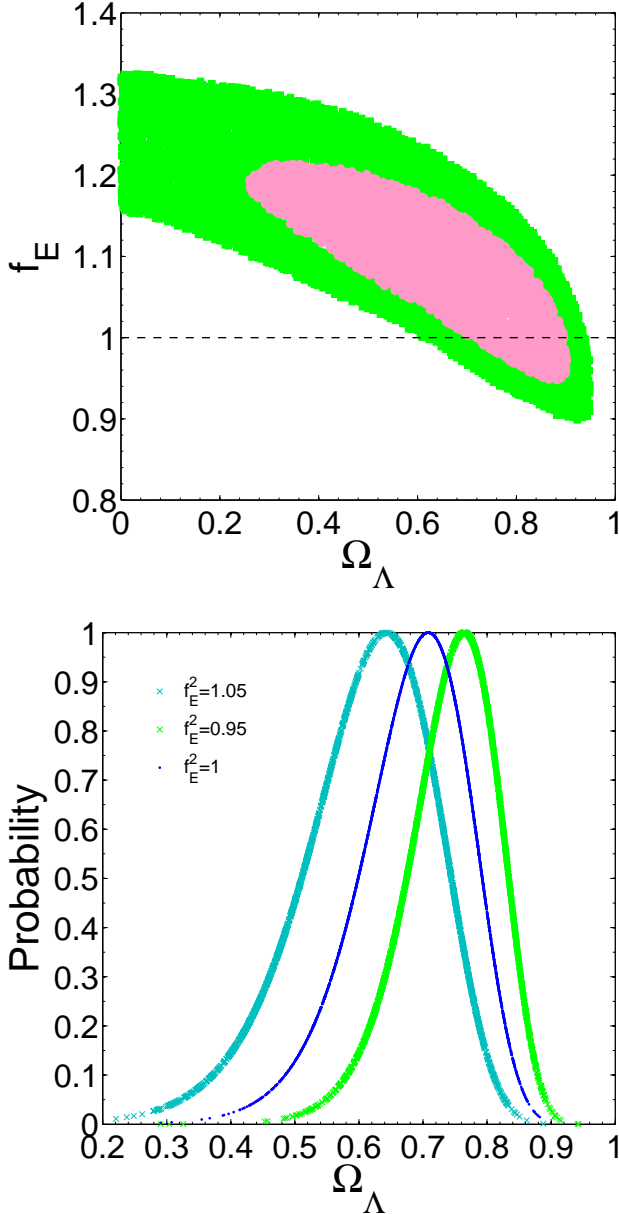


Figure 8. Upper panel: constraint results on the cosmological constant Ω_Λ and the parameter f_E for the flat Λ CDM model with the full sample ($n = 122$ lenses). The horizontal dashed line indicates the fiducial value $f_E = 1$ assumed in the paper. Lower panel: constraints on Ω_Λ with different values of f_E considering a fiducial error of $\sim 5\%$ on the values of image separations.

and the detailed luminosity profiles of galaxies.

Hence, we introduce the parameter f_E that combines the velocity dispersion σ_{SIS} and the stellar velocity dispersion σ_0

$$\sigma_{SIS} = f_E \sigma_0, \quad (21)$$

The Einstein radius given by Equation 10 is then modified as (Kochanek 1992; Ofek, Rix & Maoz 2003):

$$\Delta\theta_* = 8\pi \left(\frac{\sigma_*}{c}\right)^2 \frac{D_{ls}}{D_s} f_E^2. \quad (22)$$

More specifically, we have kept f_E as a free parameter to mimic the following effects of: (1) systematic errors in the difference between σ_0 and σ_{SIS} ;

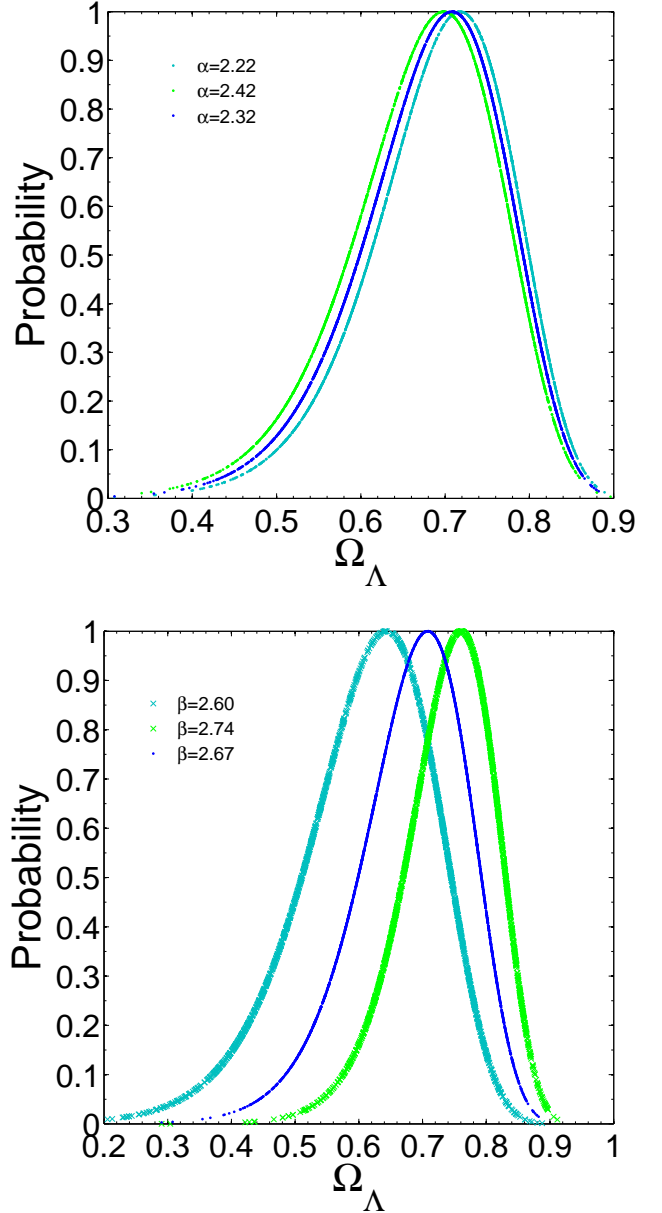


Figure 9. Normalized likelihood plot for the flat Λ CDM model with the full sample ($n = 122$ lenses), by introducing the uncertainties on the VDF parameters: the faint-end slope α and the high-velocity cut-off β , as listed in Table 3.

(2) the influence of line-of-sight mass contamination (Keeton, Kochanek, & Seljak 1997); (3) softened isothermal sphere model which may change the typical image separations (Narayan & Bartelmann 1996); and (4) the effect of secondary lenses on observed image separation. Recently, by combining stellar kinematics (central velocity dispersion measurements) with lensing geometry (Einstein radius determination from position of images), Cao et al. (2012) have tested a combined gravitational lens data set including 70 data points from SLACS and LSD, and obtained constraints on f_E consistent with the previous results (Ofek, Rix & Maoz 2003).

We consider the flat Λ CDM model and obtain simultaneous constraints on Ω_Λ and f_E with the full sample ($n = 122$ lenses). The constraint result is shown in Fig-

Table 3

Summary of the Priors and Standard Systematic Allowances Included in the Analysis.

| Parameter | Allowance |
|--|-----------------------------------|
| EoS of DE (w) | $-5 < w < 0$ |
| DE density in XCDM (Ω_x) | $0 < \Omega_x < 1$ |
| DE density in Λ CDM (Ω_Λ) | $0 < \Omega_\Lambda < 1$ |
| Matter density (Ω_m) | $0 < \Omega_m < 1$ |
| Evolution of n_* (P) | $-10 < P < 10$ |
| Evolution of σ_* (U) | $-1 < U < 1$ |
| Normalization factor (f_E) | $(0.5)^{1/2} < f_E < (2.0)^{1/2}$ |
| Faint-end slope (α) | $\alpha = 2.32 \pm 0.10$ |
| High-velocity cut-off (β) | $\beta = 2.67 \pm 0.07$ |

ure 8, with the marginalized constraints $f_E = 1.08 \pm 0.14$ and $\Omega_\Lambda = 0.65^{+0.35}_{-0.45}$. It is obvious that the cosmological constraint on Ω_Λ becomes much weaker, though the concordance Λ CDM is still favored within 1σ error region. A vanishing cosmological constant is still ruled at 1σ .

The slightly larger value of f_E indicates that larger Ω_Λ is preferred by the lens statistics with $f_E = 1$ used in this paper. This tendency is consistent with the previous result of Oguri et al. (2012) and may help explain why the observed image separation seems to be higher than model predictions (Capelo & Natarajan 2007). However, we find that the $f_E = 1$ case still consists with the data better to than 2σ . To be more specific, in order to take into account the measurement uncertainty and the approximations we are doing (no lens ellipticity accounted and no external shear), we estimate a fiducial error of $\sim 5\%$ on the values of image separations (Grillo et al. 2008), which is equivalent to a $\sim 5\%$ uncertainty on the parameter f_E^2 .

The velocity distribution function given by Equation 6 is another important source of systematic error on the final results. While adopting the best-fit values of the VDF measurement in the SDSS Data Release 5 by Choi et al. (2007) as our fiducial model, we investigate how the cosmological results are altered by introducing the uncertainties on α and β as listed in Table 3. With the results of measurements on the VDF, we vary the parameter of interest while fixing the other parameters at their best-fit values. For example, based on the $n = 122$ sample, we vary the faint-end slope α by ± 0.10 and find that this effect is quite negligible when compared to the present accuracy of the test (Mitchell et al. 2005).

The complete set of standard priors and allowances included in the analysis of the above systematics is summarized in Table 3. As shown in Figure 8 and 9 and Table 4, by comparing their contribution to the systematic error on Ω_Λ for the flat Λ CDM with the full sample, we find that the largest sources of systemic error are the dynamical normalization f_E and the high-velocity cutoff β , followed by the faint-end slope α of the VDF. This finding is consistent with the earlier results in Oguri et al. (2012). Meanwhile, this result is also compatible to the concordance cosmological model ($\Omega_\Lambda \sim 0.7$, and $\Omega_m \sim 0.3$). Indeed, current samples of lenses do not allow to discriminate between an Ω_Λ and a dynamical dark energy component.

5. CONCLUSION AND DISCUSSION

Table 4

Constraint Results Obtained by the Full Sample ($n = 122$ lenses) for the Flat Λ CDM Model with Different Systematic Errors.

| Systematics | Ω_Λ |
|---|---|
| $f_E^2 = 1.00; \alpha = 2.32; \beta = 2.67$ | $\Omega_\Lambda = 0.71^{+0.07}_{-0.08}$ |
| $f_E^2 = 0.95; \alpha = 2.32; \beta = 2.67$ | $\Omega_\Lambda = 0.76^{+0.06}_{-0.07}$ |
| $f_E^2 = 1.05; \alpha = 2.32; \beta = 2.67$ | $\Omega_\Lambda = 0.65^{+0.08}_{-0.12}$ |
| $f_E^2 = 1.00; \alpha = 2.22; \beta = 2.67$ | $\Omega_\Lambda = 0.72^{+0.08}_{-0.09}$ |
| $f_E^2 = 1.00; \alpha = 2.42; \beta = 2.67$ | $\Omega_\Lambda = 0.70^{+0.08}_{-0.10}$ |
| $f_E^2 = 1.00; \alpha = 2.32; \beta = 2.60$ | $\Omega_\Lambda = 0.64^{+0.10}_{-0.10}$ |
| $f_E^2 = 1.00; \alpha = 2.32; \beta = 2.74$ | $\Omega_\Lambda = 0.76 \pm 0.07$ |

Since the discovery of the accelerating expansion of the universe, in addition to the standard Λ CDM cosmological model, a large number of theoretical scenarios have been proposed for the acceleration mechanism. Examples include the quintessence (Ratra & Peebles 1988; Caldwell et al. 1998), phantom (Caldwell et al. 2002), quintom (Feng et al. 2005, 2006; Guo et al. 2005) and the Chaplygin gas (Kamenshchik et al. 2001; Bento et al. 2002; Alam et al. 2003; Zhu 2004; Zhang & Zhu 2006). All these acceleration mechanisms should be tested with various astronomical observations such as SNeIa, WMAP (Komatsu et al. 2009) and BAO (Percival et al. 2007). However, it is still important to use as many as different observational probes to set constraints on the cosmological parameters. In this work, we have followed this direction and used the redshift distribution of two well-defined samples of lensing, elliptical galaxies drawn from a large catalog of 122 gravitational lenses from a variety of surveys (see Table 1). The BIC is also applied in this analysis to assess various dark energy models and make a comparison.

Considering the two cases with and without the redshift evolution of the velocity function of galaxies, we have analyzed four dark energy models (the Λ CDM, the XCDM with constant w , the DGP and the RDE models) under a flat universe assumption. For each model, we have calculated the best-fit values of its parameters and found its Δ BIC value. Results are plotted in Figure 1-6.

The fit and information criteria results are summarized in Table 5. It is shown that for the zero-curvature Λ CDM model, the likelihood is maximized, for $\Omega_\Lambda = 0.70 \pm 0.09$ with no redshift evolution and $\Omega_\Lambda = 0.73 \pm 0.09$ with redshift evolution, when using the Sample A (see Section 2). Consistent results (within 1σ) are derived when the alternative Sample B is considered.

We have also derived simultaneous constraints on the redshift evolution of the parameters n_* and σ_* of the velocity function. The constraints in the $P - U$ plane also indicate that the data are consistent with the no-redshift-evolution case ($P = 0; U = 0$) at 1σ , with $P = -1.2 \pm 1.4$ and $U = 0.22^{+0.26}_{-0.27}$. Both in the no-evolution and galaxy evolution scenario, we rule out with high confidence a vanishing cosmological constant, with both the lens samples (at confidence larger than $\sim 4\sigma$), as recently found by Oguri et al. (2012) by adopting a smaller and independent lens sample. Therefore, the redshift test adds an independent evidence to the accelerating expansion.

The obtained likelihood distributions shown in Figure 1 are also in agreement with the results from an-

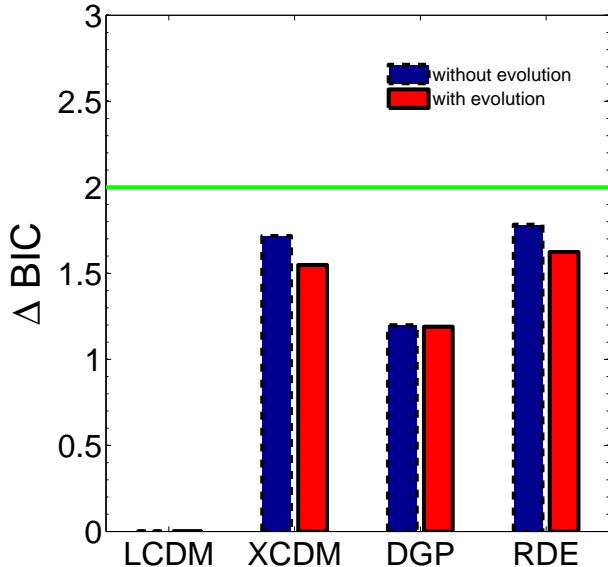


Figure 10. Graphical representation of the values of ΔBIC for each model, relative to the ΛCDM (ΛCDM). The horizontal green line indicates $\Delta\text{BIC}=2$, which is considered positive evidence against the model with the higher BIC.

Table 5

Summary of the constraint results and information criterion with Sample A. The ΔBIC values for all other models are measured with respect to the ΛCDM model.

| Model | Constraint result | ΔBIC |
|---|--|--------------------|
| ΛCDM ($P = U = 0$) | $\Omega_\Lambda = 0.70 \pm 0.09$ | 0 |
| ΛCDM ($P \neq U \neq 0$) | $\Omega_\Lambda = 0.73 \pm 0.09$ | 0 |
| XCDM ($P = U = 0$) | $\Omega_x = 0.77 \pm 0.17; w = -2.3_{-2.7}^{+1.3}$ | 1.72 |
| XCDM ($P \neq U \neq 0$) | $\Omega_x = 0.79 \pm 0.13; w = -2.1_{-2.8}^{+1.1}$ | 1.55 |
| DGP ($P = U = 0$) | $\Omega_m = 0.25_{-0.09}^{+0.11}$ | 1.20 |
| DGP ($P \neq U \neq 0$) | $\Omega_m = 0.22_{-0.09}^{+0.10}$ | 1.19 |
| RDE ($P = U = 0$) | $\Omega_m = 0.22_{-0.11}^{+0.10}; \beta = 0.29 \pm 0.19$ | 1.78 |
| RDE ($P \neq U \neq 0$) | $\Omega_m = 0.18_{-0.12}^{+0.11}; \beta = 0.28 \pm 0.18$ | 1.62 |

alyzing data of WMAP 5-year results with the BAO and SNe Union data, and the large-scale structures in the SDSS luminous red galaxies (Spergel et al. 2003; Tegmark et al. 2004; Eisenstein et al. 2005), which implies that gravitational lensing statistics provides an independent and complementary support on the ΛCDM model.

We give a graphical representation of the BIC test Figure 10. Following the ΛCDM model, the DGP model is the only one-parameter model that reduces to the ΛCDM but gives a worse fit, as we obtained close values for the matter density. The XCDM model gives a comparably good fit, but has one additional free parameter, that is in accordance with the best-fit ΛCDM model (within 1σ range for the EoS parameter). The other two-parameter model, RDE, provides a worst fit to the data, though the difference in BIC (ΔBIC) indicates no clear evidence against it. Therefore, while still not firmly ruling out competing world models, the redshift distribution test clearly favors the cosmological constant model, a conclusion in accordance with previous works (Davis et al. 2007).

In order to assess the reliability of our results and the related systematic errors, we have introduced three additional lens samples, characterized by different degrees of inhomogeneity and incompleteness, and re-derived an estimate for the cosmological constant assuming a not evolving lens population. Two lens samples (the whole heterogeneous catalog of 122 systems and the SLACS sample) give results fully consistent with those discussed above, confirming us that systematic errors due to sample selection are not larger than statistical uncertainties.

Our model involves several uncertainties and assumptions that introduce additional systematic errors in our cosmological analysis (see Table 3). By comparing the contribution of each of these systematic errors to the systematic error on the flat ΛCDM model (see Figure 8 and 9 and Table 4), we find that the largest sources of systematic error are the dynamical normalization and the high-velocity cutoff factor, followed by the faint-end slope of the velocity dispersion function, which is consistent with the earlier results in Oguri et al. (2012). Moreover, the comparable systematic errors suggest the importance of careful studies of the systematics for robust cosmological constraints from lens statistics.

Finally, we note that four important effects should be mentioned. Evolution of the source population can also matter the technique applied in this paper, which might have a small second-order effect on the statistics (Oguri et al. 2012). We have also neglected systematic uncertainties due to the effect of small-scale inhomogeneities on large-scale observations. In fact, the inhomogeneous matter distribution can affect light propagation and the related cosmological distances (Serenio et al. 2001, 2002), although its effect on the total lensing statistics is small (Covone et al. 2005). Meanwhile, the lens redshift test applied in this paper may also lose the statistical power of absolute lensing probabilities. The last one is, multiple errors or biases in the method could easily be canceled out, which may lead the result to be a statistical fluke (Maoz 2005).

Despite some of its inherent difficulties, the redshift distribution test, with either larger gravitational lensing samples from future wide-field surveys such as Pan-STARRS and Large Synoptic Survey Telescope by taking advantage of time-domain information (Oguri & Marshall 2010) or a joint investigation with other cosmological observations, could be helpful for advancing such applications and provide more stringent constraints on the cosmological parameters.

We acknowledge fruitful discussions with M. Paolillo. We thank the anonymous referee for his/her valuable comments which helped us to improve the paper. GC thanks I. Skripnikova for enlightening discussions. This work was supported by the National Natural Science Foundation of China under the Distinguished Young Scholar Grant 10825313 and Grant 11073005, the Ministry of Science and Technology national basic science Program (Project 973) under Grant No. 2012CB821804, the Fundamental Research Funds for the Central Universities and Scientific Research Foundation of Beijing Normal University, and the Excellent Doctoral Disserta-

tion of Beijing Normal University Engagement Fund.

REFERENCES

- Alam, U., Sahni, V., Saini, T. D., & Starobinsky, A. A. 2003, *MNRAS*, 334, 1057
- Alcaniz, J. S. 2002, *PRD*, 65, 123514
- Alcaniz, J. S., Jain, D., & Dev, A. 2003, *PRD*, 67, 043514
- Amani, A. R. 2011, *Int J Theor Phys*, 50, 3078
- Anguita, T., Faure, C., Kneib, J.-P., Wambsganss, J., Knobel, C., Koekemoer, A. M., & Limousin, M. 2009, *A&A*, 507, 35
- Arneson, R. A., Brownstein, J. R., Bolton, A. S. 2012, *ApJ*, 753, 4
- Bennett, C. L., et al. 2003, *ApJS*, 148, 1
- Bento, M. C., Bertolami, O., & Sen, A. A. 2002, *PRD*, 66, 043507
- Biesiada, M., Piórkowska, A., & Malec, B. 2010, *MNRAS*, 406, 1055
- Biggs, A. D., et al. 2003, *MNRAS*, 338, 1084
- Blackburne, J. A., Wisotzki, L., & Schechter, P. L. 2008, *AJ*, 135, 374
- Bolton, A. S., et al. 2008, *ApJ*, 682, 964
- Brown, M. J. I., et al. 2007, *ApJ*, 654, 858
- Burud, I., et al. 2002a, *A&A*, 383, 71
- Burud, I., et al. 2002b, *A&A*, 391, 481
- Caldwell, R., Dave, R., & Steinhardt, P. J. 1998, *PRL*, 80, 1582
- Caldwell, R. 2002, *PLB*, 545, 23;
- Cao, S., Zhu, Z.-H., & Liang, N. 2011, *A&A*, 529, A61
- Cao, S., Liang, N., & Zhu, Z.-H. 2011, *MNRAS*, 416, 1099
- Cao, S., Zhu, Z.-H., & Zhao, R. 2011, *PRD*, 84, 023005
- Cao, S., & Zhu, Z.-H. 2012, *A&A*, 538, A43
- Cao, S., et al. 2012, *JCAP*, 03, 016
- Capelo, P. R., & Natarajan, P. 2007, *NJPh*, 9, 445
- Chae, K.-H., et al. 2002, *PRL*, 89, 151301
- Chae, K.-H. 2003, *MNRAS*, 346, 746
- Chae, K.-H. 2007, *ApJL*, 658, L71
- Chiba, M., & Yoshii, Y. 1999, *ApJ*, 510, 42
- Choi, Y.-Y., Park, C., & Vogeley, M. S. 2007, *ApJ*, 884, 897
- Cohen, J. G., Lawrence, C. R., & Blandford, R. D. 2003, *ApJ*, 583, 67
- Cohn, J. D., & Kochanek, C. S. 2004, *ApJ*, 608, 25
- Cooray, A. R., & Huterer, D. 1999, *ApJ*, 513, L95
- Covone, G., Sereno, M., & de Ritis, R. 2005, *MNRAS*, 357, 773
- Crampton, D., Schade, D., Hammer, F., Matzkin, A., Lilly, S. J., & Le Fèvre, O. 2002, *ApJ*, 570, 86
- Davis, T. M., et al. 2007, *ApJ*, 666, 716
- Durrer, R., & Maartens, R. 2010, "Dark Energy: Observational & Theoretical Approaches", ed. P Ruiz-Lapuente (Cambridge UP), pp 48-91 [arXiv:0811.4132]
- Dvali, G., Gabadadze, G., & Porrati, M. 2000, *PLB*, 485, 208
- Eigenbrod, A., Courbin, F., Meylan, G., Vuissoz, C., & Magain, P. 2006, *A&A*, 451, 759
- Eisenhardt, P. R., Armus, L., Hogg, D. W., Soifer, B. T., Neugebauer, G., & Werner, M. W. 1996, *ApJ*, 461, 72
- Eisenstein, D. J., et al. 2005, *ApJ*, 633, 560
- Faber, S. M., et al. 2007, *ApJ*, 665, 265
- Falco, E. E., Lehár, J., & Shapiro, I. I. 1997, *AJ*, 113, 540
- Fang, W., Wang, S., Hu, W., Haiman, Z., Hui, L., & May, M. 2008, *PRD*, 78, 103509
- Fassnacht, C. D., et al. 1996, *ApJL*, 460, L103
- Fassnacht, C. D., & Cohen, J. G. 1998, *AJ*, 115, 377
- Fassnacht, C. D., et al. 1999, *AJ*, 117, 658
- Faure, C., et al. 2008, *ApJS*, 176, 19
- Faure, C., et al. 2009, *ApJ*, 695, 1233
- Faure, C., et al. 2011, *A&A*, 529, A72
- Feng, B., Wang, X., & Zhang, X. 2005, *PLB*, 607, 35
- Feng, B., Li, M., Piao, Y., & Zhang, X. 2006, *PLB*, 634, 101
- Feng, C. J., & Li, X. Z. 2009, *PLB*, 680, 184
- Fukugita, M., Futamase, T., & Kasai, M. 1990, *MNRAS*, 246, 24P
- Gao, C., et al. 2009, *PRD*, 79, 043511
- Gaztañaga, E., Cabré, A., & Hui, L. 2009, *MNRAS*, 399, 1663
- Gregg, M. D., et al. 2000, *AJ*, 119, 2535
- Gregg, M. D., et al. 2002, *ApJ*, 564, 133
- Grillo, C., Lombardi, M., & Bertin, G. 2008, *A&A*, 477, 397
- Guo, Z. K., Piao, Y., Zhang, X., & Zhang, Y. 2005, *PLB*, 608, 177
- Hagen, H.-J., & Reimers, D. 2000, *A&A*, 357, L29
- Hall, P. B., et al. 2002, *ApJ*, 575, L51
- Helbig, P., & Kayser, R. 1996, *A&A*, 308, 359
- Hewett, P. C., et al. 1994, *AJ*, 108, 1534
- Hinshaw, G., et al. 2009, *ApJS*, 180, 225
- Huchra, J., Gorenstein, M., Kent, S., Shapiro, I., Smith, G., Horine, E., & Perley, R. 1985, *AJ*, 90, 691
- Im, M., et al. 2002, *ApJ*, 571, 136
- Inada, N., et al. 2005, *AJ*, 130, 1967
- Inada, N., et al. 2008, *AJ*, 135, 496
- Johnston, D. E., et al. 2003, *AJ*, 126, 2281
- Kamenshchik, A., Moschella, U., & Pasquier, V. 2001, *PLB*, 511, 265
- Kang, X., Jing, Y. P., Mo, H. J., & Börner, G. 2005, *ApJ*, 631, 21
- Keeton, C. R., Kochanek, C. S., & Seljak, U. 1997, *ApJ*, 482, 604
- Keeton, C. R., & Zabludoff, A. I. 2004, *ApJ*, 612, 660
- Kneib, J., Cohen, J. G., & Hjorth, J. 2000, *ApJ*, 544, L35
- Kochanek, C. S. 1992, *ApJ*, 384, 1
- Kochanek, C. S. 1996a, *ApJ*, 466, 638
- Kochanek, C. S., 1996b, *ApJ* 473, 595
- Kochanek, C. S., et al. 2000, *ApJ*, 543, 131
- Komatsu, E., et al. [WMAP Collaboration], 2009, *ApJS*, 180, 330
- Koopmans, L. V. E., & Treu, T. 2002, *ApJ*, 568, L5
- Koopmans, L. V. E., & Treu, T. 2003, *ApJ*, 583, 606
- Lacy, M., Gregg, M., Becker, R. H., White, R. L., Glikman, E., Helfand, D., & Winn, J. N. 2002, *AJ*, 123, 2925
- Lagattuta, D. J., et al. 2010, *ApJ*, 716, 1579
- Langston, G. I., et al. 1989, *AJ*, 97, 1283
- Lehár, J., Langston, G. I., Silber, A., Lawrence, C. R., & Burke, B. F. 1993, *AJ*, 105, 847
- Lehár, J., et al. 2000, *ApJ*, 536, 584
- Lewis, A., & Bridle, S. 2002, *PRD*, 66, 103, 511
- Li, M., et al. 2010, *ScChG*, 53, 1631
- Lidman, C., Courbin, F., Kneib, J.-P., Golse, G., Castander, F., & Soucail, G. 2000, *A&A*, 364, L62
- Lubin, L. M., Fassnacht, C. D., Readhead, A. C. S., Blandford, R. D., & Kundić, T. 2000, *AJ*, 119, 451
- Maartens, R., & Koyama, K. 2010, *Living Rev. Relativity*, 13, 5
- Mandelbaum, R., van de Ven, G., & Keeton, C. R. 2009, *MNRAS*, 398, 2
- Maoz, D., Rix, H.-W. 1993, *ApJ*, 416, 425
- Maoz, D. 2005, *Impact of Gravitational Lensing on Cosmology* Proceedings, IAU Symposium, No.225, Eds. Y. Mellier and G. Meylan [arXiv:0501491]
- Mitchell, J. L., Keeton, C. R., Frieman, J. A., & Sheth, R. K. 2005, *ApJ*, 622, 81
- Morgan, N. D., et al. 2001, *AJ*, 121, 611
- Morgan, N. D., et al. 2004, *AJ*, 127, 2617
- Moustakas, L. A., et al. 2007, *ApJ*, 660, L31
- Muñoz, J. A., et al. 2001, *ApJ*, 546, 769
- Myers, S. T., et al. 1999, *AJ*, 117, 2565
- Narayan, R., & Bartelmann, M. 1996, In: "Lectures on Gravitational Lensing" [arXiv:9606001]
- Nemiroff, R. J. 1989, *ApJ*, 341, 579
- Newton, E., et al. 2011, *ApJ*, 734, 104 [arXiv:1104.2608]
- O'Dea, C. P., et al. 1992, *AJ*, 104, 1320
- Ofek, E. O., Rix, H.-W., & Maoz, D. 2003, *MNRAS*, 343, 639
- Ofek, E. O., Maoz, D., Rix, H.-W., Kochanek, C. S., & Falco, E. E. 2006, *ApJ*, 641, 70
- Oguri, M., Keeton, C. R., & Dalal, N. 2005, *MNRAS*, 364, 1451
- Oguri, M., & Marshall, P. J. 2010, *MNRAS*, 405, 2579
- Oguri, M., et al. 2012, *AJ*, 143, 120
- Percival, W. J., et al. 2007, *MNRAS*, 381, 1053
- Perlmutter, S., et al. 1999, *ApJ*, 517, 565
- Pires, N., Zhu, Z.-H. & Alcaniz, J. S. 2006, *PRD*, 73, 123530
- Ratnatunga, K. U., Griffiths, R. E., Ostrander, E. J. 1999, *AJ*, 117, 2010
- Ratra, B., & Peebles, P. E. J. 1988, *PRD*, 37, 3406
- Riess, A. G., et al. 1998, *AJ*, 116, 1009
- Ruff, A. J., et al. 2011, *ApJ*, 727, 96
- Schechter, P. L., Gregg, M. D., Becker, R. H., Helfand, D. J., & White, R. L. 1998, *AJ*, 115, 1371
- Schechter, P. 2004, the proceedings of IAU Symposium No. 225: The Impact of Gravitational Lensing on Cosmology, Mellier, Y. and Meylan, G. eds [arXiv:0408338]
- Schwarz, G. 1978, *Ann. Stat.* 6, 461
- Sereno, M., Covone, G., Piedipalumbo, E., & de Ritis, R. 2001, *MNRAS*, 327, 517.
- Sereno, M. 2002, *A&A*, 393, 757
- Sereno, M., Piedipalumbo, E., Sazhin, M. V. 2002, *MNRAS*, 335, 1061

- Sereno, M., & Longo, G. 2004, MNRAS, 354, 1255
Sereno, M. 2005, MNRAS, 356, 937
Sheth, R. K., et al. 2003, ApJ, 594, 225
Siemiginowska, A., Bechtold, J., Aldcroft, T. L., McLeod, K. K., & Keeton, C. R. 1998, ApJ, 503, 118
Sluse, D., et al. 2003, A&A, 406, L43
Spergel, D. N., et al. 2003, ApJS, 148, 175
Stern, D., et al. 2010, JCAP, 02, 008
Surdej, J., et al. 1997, A&A, 327, L1
Sykes, C. M., et al. 1998, MNRAS, 301, 310
Tegmark, M., et al. 2004, PRD, 69, 103
Tonry, J. L. 1998, AJ, 115, 1
Tonry, J. L., & Kochanek, C. S. 1999, AJ, 117, 2034
Treu, T., & Koopmans, L. V. E. 2004, ApJ, 611, 739
Treu, T., Koopmans, L. V. E., Bolton A. S., Burles S., & Moustakas L. A. 2006, ApJ, 640, 662
Treu, T., et al. 2009, ApJ, 690, 670
van de Ven, G., Mandelbaum, R., & Keeton, C. R. 2009, MNRAS, 398, 2
White, R. E., & Davis, D. S. 1996, American Astronomical Society Meeting, 28, 1323
Wiklind, T., & Combes, F. 1995, A&A, 299, 382
Wiklind, T., & Combes, F. 1996, Nature, 379, 139
Winn, J. N., et al. 2000, AJ, 120, 2868
Winn, J. N., et al. 2002a, AJ, 123, 10
Winn, J. N., et al. 2002b, ApJ, 564, 143
Wisotzki, L., Schechter, P. L., Bradt, H. V., Heinmüller, J., & Reimers, D. 2002, A&A, 395, 17
Yamamoto, K., & Futamase, T. 2001, Prog. Theor. Phys., 105, 707
Zhang, H., & Zhu, Z.-H. 2006, PRD, 73, 043518
Zhu, Z.-H. 1998, A&A, 338, 777
Zhu, Z.-H., & Fujimoto, M. K. 2002, ApJ, 581, 1
Zhu, Z.-H. 2004, A&A, 423, 421
Zhu, Z.-H., & Alcaniz, J. S. 2005, ApJ, 620, 7
Zhu, Z.-H., & Sereno, M. 2008, A&A, 487, 831